https://doi.org/10.33472/AFJBS.6.8.2024.141-153

African Journal of Biological Sciences

Research Paper Open Access

INVESTIGATION OF THE STRUCTURAL AND FUNCTIONAL PROPERTIES OF STARCH-G-POLY (ACRYLIC ACID) HYDROGELS REINFORCED WITH CELLULOSE NANOFIBERS FOR CU2+ ION ADSORPTION

Ankita Tripathi[1], Nakul Gupta[2], Bharti Chauhan[3], Neha Priya[4], Prakash S. Sukhramani[5], Harshad Jitubhai Trivedi[6], Mallamma T[7], Vidyashree N H[8], Rajesh Dodiya*[9], Keshamma E[10], Suraj Mandal[11]

[1]Associate Professor, IIMT College of Pharmacy, Greater Noida, UP

[2]Director & Professor, IIMT College of Pharmacy, Greater Noida, UP

[3,4]Assistant Professor, IIMT College of Pharmacy, Greater Noida, UP

[5]Professor and HOD (Pharmaceutics), Veerayatan Institute of Pharmacy, Bhuj-Mandvi Road, Jakhania, Mandvi, Kutch, Gujarat- 370465, India

[6]Assistant Professor, D. L Patel Science College Vidhyanagari Himatnagar 383001

[7]Assistant Professor, Sri Adichunchanagiri College of Pharmacy, Adichcunchanagiri University

[8]Assistant Professor, Nitte College of Pharmaceutical sciences, Bangalore

[9]Associate Professor, School of Pharmacy, Parul University

[10]Associate professor, Department of Biochemistry, Maharani Cluster University, Bengaluru-560001, Karnataka, India.

[11]Assistant Professor, Department of Pharmacy, IIMT College of Medical Sciences, IIMT University, O-Pocket, Ganganagar, Meerut, 250001, U.P., India

Corresponding Author Details:

Rajesh Dodiya, Associate Professor, School of Pharmacy, Parul University

Email: rajdodia7@gmail.com

Article History

Volume 6,Issue 8, 2024

Received:20 Feb 2024

Accepted : 28 Mar 2024

doi: 10.33472/AFJBS.6.8.2024.141-153

Abstract

To really adsorb Cu2+ particles from watery arrangements, this study analyzes the underlying and useful qualities of starch-g-poly (acrylic corrosive) (St-g-PAA) hydrogels supported with cellulose nanofibers (CNFs). To further develop recuperation and reuse, the review examines the creation of composite hydrogels containing attractive nanoparticles (Fe3O4) included expansion to starch, acrylic corrosive, and CNFs. A scope of characterisation techniques were used to examine the synthetic construction, morphology, and basic substance of the hydrogels both before to and during Cu2+ adsorption, like FTIR spectroscopy, SEM investigation, and component sythesis examination. Also, vibrating test magnetometry was utilized to analyze the attractive qualities of attractive hydrogels and Fe3O4 nanoparticles. The outcomes show that the hydrogels went through significant morphological and synthetic changes after Cu2+ adsorption, with the consideration of attractive nanoparticles and CNFs being answerable for the expanded adsorption ability. The work gives bits of knowledge into the primary properties and practical limits of these composite hydrogels in water treatment applications, featuring their true capacity for productive expulsion of weighty metal particles from water sources.

Keywords: *Cu2+ ion adsorption, starch-g-poly(acrylic acid) hydrogels, cellulose nanofibers, magnetic nanoparticles, structural characteristics*

1. INTRODUCTION

Industrial water pollution presents serious environmental problems, especially when it comes to colours and heavy metals poisoning streams [1]. These contaminants endanger human health in addition to harming aquatic life [2]. As a result, it is imperative to lessen their effects, particularly in sectors like food processing and agriculture [3]. There are several ways to remove heavy metals from water, but polymeric adsorbents are becoming more popular because of how efficient, easy to use, and reusable they are [4]. Water treatment applications can benefit greatly from the natural availability and biocompatibility of biopolymers like cellulose and keratin [5].

Using synthetic polymers like poly(acrylic acid) and biopolymers like cellulose to create hydrogels is one promising method [6]. These hydrogels can be customized for certain contaminants and have large surface surfaces for adsorption [7]. These hydrogels' structural integrity and adsorption ability are improved by the addition of cellulose nanofibers, especially for heavy metal ions like Cu2+ [8]. Furthermore, new developments involve the easy recovery and reuse following treatment by mixing hydrogels with magnetic nanoparticles, like Fe3O4 [9]. This invention solves the problem of adsorbent retrieval from aqueous solutions in addition to increasing adsorption efficiency[10].

Several synthesis techniques and characterizations have been investigated in this field of study to maximize the functionality of these hybrid hydrogels [11-13]. These investigations have yielded encouraging findings, suggesting that cellulose nanofiber-reinforced starch-g-poly(acrylic acid) hydrogels may be useful for effective Cu2+ ion adsorption in water treatment applications [14]. All things considered, learning more about the structural and functional

characteristics of these composite hydrogels provides opportunities for long-term, practical solutions to the problem of heavy metal contamination of water supplies [15 -16].

1.1.Research objectives

- To improve the cellulose nanofiber (CNF) reinforced starch-g-poly(acrylic acid) hydrogel production process.
- To determine the structural characteristics of the produced nanocomposite hydrogels by employing methods like SEM imaging and FTIR spectroscopy.
- To examine the hydrogels' functional characteristics, paying special attention to how well they can adsorb Cu2+ ions.
- To analyze how adding Fe3O4 nanoparticles affected the hydrogels' structural and functional characteristics, such as their magnetic qualities and their ability to adsorb Cu2+ ions with efficiency.

2. LITERATURE REVIEW

Dragan et al., (2014) have developed composite chelating sorbents for effective Cu2+ ion sorption in water treatment applications. The sorbent material used is potato starch-graft-polyamidoxime (PS-g-PAO) embedded in chitosan beads. This aligns with the trend towards biopolymers for environmental restoration [17]. The grafted polyamidoxime enhances the starch's chelating properties. The chitosan biopolymer provides structural support and simplifies handling. The study emphasizes the need for continuous innovation in water treatment technology and the importance of effective sorption materials in combating heavy metal pollution.

Chen et al. (2022) explores the creation of an efficient Cu2+ ion adsorbent using a modified kaolin hydrogel. This study supports the increasing interest in using naturally occurring minerals, including kaolin, because of its affordability and abundance for environmental remediation [18]. Clay minerals such as kaolin have intrinsic adsorption qualities because of their high surface area and porous nature. In order to improve kaolin's adsorption ability and stability in aquatic conditions, functional groups or polymers are added to the material to transform it into a hydrogel. This method emphasizes how crucial it is to customise materials for certain contaminants in order to attain the highest level of removal efficiency. Through investigating kaolin modification for Cu2+ adsorption, the study tackles the need for long-term and economically viable ways to reduce heavy metal contamination in water sources. Furthermore, this research advances knowledge about hydrogel-based adsorbents and their possible uses in environmental cleanup. All things considered, Chen and colleagues' study offers insightful information to the continuing attempts to create novel adsorption materials for water treatment applications.

Renani et al., (2023) have developed magnetic nano-biocomposite hydrogels as advanced materials for removing Cu2+ ions from aqueous solutions. These hydrogels, made from starch-g-poly(acrylic acid) and cellulose nanofibers, are designed for efficient pollutant removal. The inclusion of magnetic nanoparticles enhances the hydrogel's recovery and reuse, a challenge in water treatment processes [19]. The study underscores the potential of biocomposite hydrogels in addressing heavy metal pollution and contributes to sustainable water remediation efforts. The application of magnetic nanoparticles in hydrogel-based adsorbents also opens up new avenues in environmental nanotechnology.

Baghbadorani et al., (2019) have fostered a superadsorbent hydrogel utilizing cellulose nanofibers and starch-g-poly(acrylic corrosive) as a spine polymer. The hydrogels are intended to eliminate Cu2+ particles from fluid arrangements, upgrading their primary trustworthiness and adsorption limit. The review stresses the significance of streamlining material organization for designated toxin expulsion [20]. The examination expands on past examinations in superadsorbent hydrogels, stressing the meaning of cellulose nanofibers as supporting specialists. The discoveries add to the comprehension of cellulose-based materials in water treatment applications and feature their true capacity as compelling adsorbents for weighty metal particles.

3. RESEARCH METHODOLOGY

3.1.Materials

Insightful grades were applied to the starch ((C6H10O5)n·(H2O)), potassium persulfate (K2SO4), acrylic corrosive (AA), sodium hydroxide (NaOH), and N,N′-methylene bisacrylamide (MBA) that were gained from Merck, Germany. CNFs got from a softwood source utilizing a chemo-mechanical strategy were provided by Nano Novin Polymer Co. (Sari, Iran). We purchased attractive nanoparticles (Fe3O4) from the Sigma-Aldrich Organization. Cu(SO4)2H2O was procured from Merck Organization in Germany to set up a Cu2+ stock arrangement with a centralization of 600 ppm.

3.2.M-St-g-P(AA)/CNFs Hydrogel Bioadsorbent Synthesis

The St-g-P(AA)/CNFs composite was ready by adding starch to refined water in a four-necked reactor. The arrangement was then warmed to 85-95°C for 60 minutes, trailed by adding potassium persulfate as an initiator. An answer containing refined water, MBA as a crosslinker, AA as a monomer, and CNFs was progressively filled the reactor for extremist polymerization. The hydrogels were then submerged in a basic arrangement, and unreacted material was dispensed with by drenching them in ethanol, expanding them in refined water, and afterward being saturated with ethanol once more. The hydrogel mass was dried in a broiler until a steady weight was reached.

The addition of Fe3O4 nanoparticles (2 and 8 weight percent AA monomer content) during the combination allowed for the incorporation of an appealing hydrogel. The appealing nanoparticles were sonicated for 10 minutes in a solution that included a monomer, cellulose nanofibers, and a crosslinker. Subsequently, they were gently added to the reaction mixture. Hydrogels were ready in mass and powder structures to think about their capacity for metal particle adsorption. The hydrogel powder was ground utilizing a high-energy ball factory.

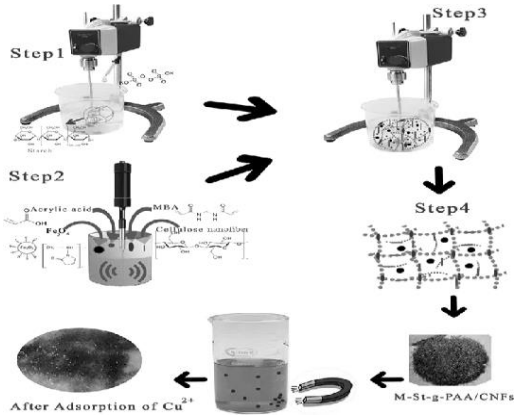

Figure 1: Steps in the M-St-g-PAA/CNF synthesis.

3.3.Characterization of the Synthesized Adsorbents

FTIR spectroscopy was utilized to inspect the synthetic design of the created nanocomposite hydrogel adsorbents. For utilization in the 4000-500 cm-1 recurrence area of the FTIR spectrometer (Bruker Tensor 27, Germany), the powdered hydrogel tests were mixed with KBr and from there on shaped into plates. Utilizing imaging electron microscopy (SEM) pictures produced by a FEI Quanta 200 model and energy dispersive X-ray spectroscopy (EDX), the hydrogels' design, structure, and key changes with Cu2+ molecule adsorption were examined. We used vibrating test magnetometry (VSM; MDKB) to assess the desirable features of the integrated adsorbent.

3.4.Adsorption of Cu^{2+}

Various arrangements of Cu2+ particles with changing focuses (0.4-0.6 g/L) were utilized to assess the expulsion of the Cu2+ particles from the watery arrangement by hydrogels; 0.05 g of every hydrogel was plunged into 50 mL of every arrangement at pH = 5 (see Area 3.6). Condition 1 was utilized to figure the amount of Cu2+ adsorbed just barely of nanocomposite hydrogels at 25 °C. When the arrangements were separated and the balance state was reached, the convergence of Cu2+ particles was resolved utilizing a solitary bar spectrophotometer (UV-Vis, Shimadzu 240 model, Japan) with a frequency of λ = 620 nm. We utilized alkali answer for further develop the variety power of copper arrangements and to all the more definitively show more noteworthy retention in the apparent region. The accompanying condition was utilized to make an adjusted bend that yielded the particle focuses for the various examples (R2 > 0.998).

$$q = \frac{(C_0 - C_e)}{m} V \qquad (1)$$

and the Cu^{2+} evacuation effectiveness rate was determined by the accompanying: where m is the hydrogel weight (g), V is the plan's volume (L), q is as far as possible at balance (mg/g), and C0 and Ce are the hidden and congruity unions of Cu2+ (mg/L), exclusively.

$$\%\, removal = \frac{(C_0 - C_e)}{(C_0)} \times 100 \qquad (2)$$

3.5.Swelling Measurement

At room temperature, a predetermined amount of hydrogel was immersed in a 50 mL water mixture with varying pH values (2, 7, and 11). Adjusting the pH of the mixture with HCl and NaOH allowed us to zero down on the expanding conduct of the hydrogel. The expanded gel was eliminated from the medium at customary stretches, and in the wake of utilizing channel paper to eliminate any excess water, its weight was recorded. Until the expanding gel arrived at a consistent weight, the interaction was rehashed. Utilizing: the enlarging proportion (S) was figured.

$$S = \frac{W_s - W_d}{W_d} \qquad (3)$$

where Ws and Wd represent the hydrogels' general loads in the wake of expanding and drying.

From the expanding proportion (S) versus time plot, the enlarging rate (SR) and balance expanding (Se) were determined utilizing.

$$S_t = S_e\left(1 - e^{-t/r}\right) \qquad (4)$$

where τ (min) is the rate boundary and St (g/g) and Se (g/g) are the expanding proportions at time t and balance time, individually. The accompanying condition was utilized to compute the hydrogel's expanding rate (SR) (g/(g·min)) at different pH values:

$$SR = \frac{S_\tau}{\tau} \qquad (5)$$

where Sτ (g/g) is the enlarging at time τ (min).

4. RESULTS AND DISCUSSION

4.1.FTIR Spectroscopy

The audit zeroed in on the starch-g-poly(acrylic destructive) and engaging starch-g-poly(acrylic destructive) nanocomposite hydrogels, as well as the intermolecular engineered organizations in these hydrogels. At the point when Cu2+ was adsorbed, FTIR spectroscopy was utilized to examine the subsequent spectra. The (−OH) extending vibration was credited to the expansive band at 3300-3500 cm-1, though the critical mark band inside the 1500-1650 cm-1 zone showed −OH winding in all cases. The noticed changes and developments propose a metal-including collaboration through molecule exchange and chelation happening on the outer layer of the examples between carboxyl groups (COOH), carboxylate groups (COO-), and Cu2+ particles. Due to the extended vibrations of C and C-O lopsided pyran rings, as well as the mutilated vibrations of C-O-C, the melding of CNFs inside the matrix brought about extra tops at 1056 cm-1, 1037 cm-1, 1045 cm-1, and 1039 cm-1. There is a relationship between's the vibration of Fe-O and the band seen at 422 cm-1 in the FTIR range of Fe3O4. Nonetheless, following Cu2+ adsorption on the nanoparticle surface and the genuine effect, the Fe-O signature top in the appealing hydrogel was moved to a lower wavenumber.

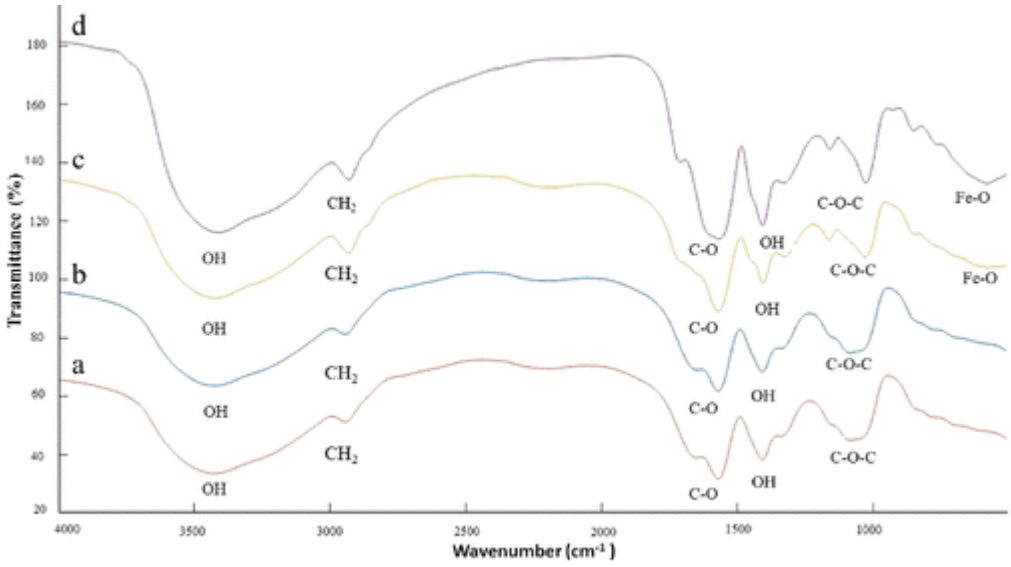

Figure 2: Coming up next are the FTIR spectra of the hydrogels: (a) St-g-P(AA)/CNFs, (b) St-g-P)AA(/CNFs hydrogels following Cu2+ adsorption, (c) M-St-g-PAA/CNFs, and (d) M-St-g-PAA hydrogels following Cu2+ adsorption.

4.2.Morphology of the Adsorbent

SEM examination was utilized to look at the morphological changes in the hydrogel both when the adsorption of Cu2+. Tests for St-g-PAA/CNFs and M-St-g-PAA/CNFs, as displayed in Figure 3 a,b, show a lopsided permeable design before adsorption. An organization structure is made by the associations between these pores. Water atoms and different particles have

utilitarian pathways to enter and leave the hydrogel all the more effectively on the grounds that to this organization like construction. It is obvious that the state of the holes in hydrogels has been extensively adjusted by Cu2+ particle adsorption. It is essential to take note of that when Cu2+ particles were adsorbed, the hydrogels turned out to be more fragile and unpleasant.

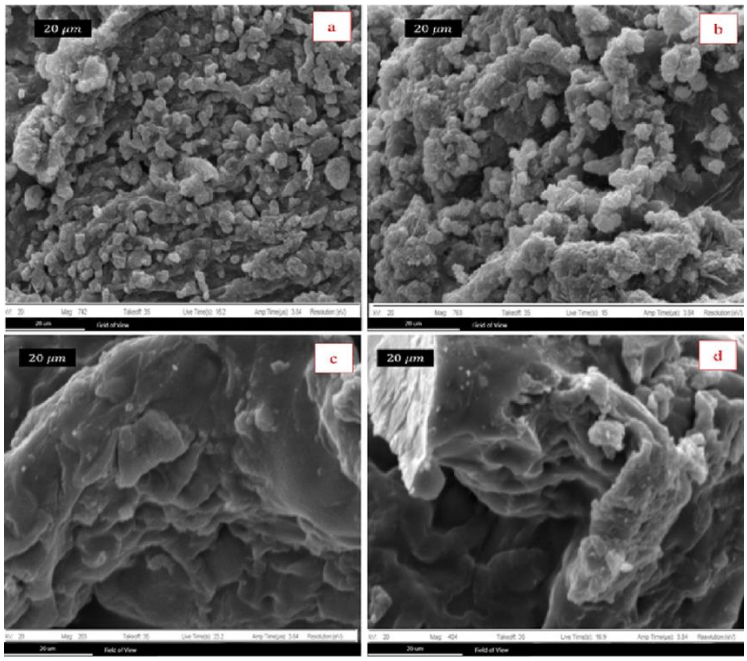

Figure 3: EM pictures of the accompanying things: Here are the M-St-g-PAA/CNFs and St-g-PAA/CNFs before adsorption, as well as the St-g-PAA/CNFs and M-St-g-PAA/CNFs after Cu2+ adsorption.

Table 1(a): Element Composition Analysis

Element	Weight%	Atomic %
CK	30.01	41.50
Ok	57.45	55.45
SK	7.29	3.65

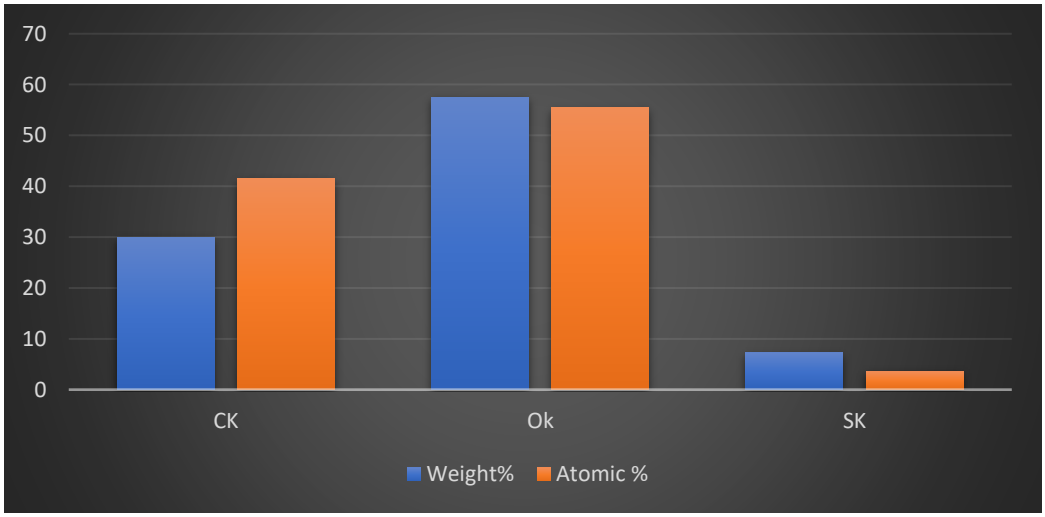

Figure 4 (a): Graphical representation on the percentage of Element Composition Analysis Three elements—CK, Ok, and SK—have weight and atomic percentages shown. CK, which contains Calcium and Potassium, has a weight percentage of 30.01% and an atomic percentage

of 41.50%. This means that in the sample under inspection, CK accounts for 30.01% of all element weight and 41.50% of atom count. Ok, signifying Oxygen and Potassium, has a weight percentage of 57.45% and an atomic percentage of 55.45%. This means Ok makes up 57.45% of the sample's weight and 55.45% of its atomic makeup. SK has a weight proportion of 7.29% and an atomic percentage of 3.65%. SK appears to be lighter and less atomically composed than the other elements.

Table 1 (b): Element Composition Analysis

Element	Weight%	Atomic %
CK	22.32	11.45
Ok	35.64	35.11
SK	56.11	45.22

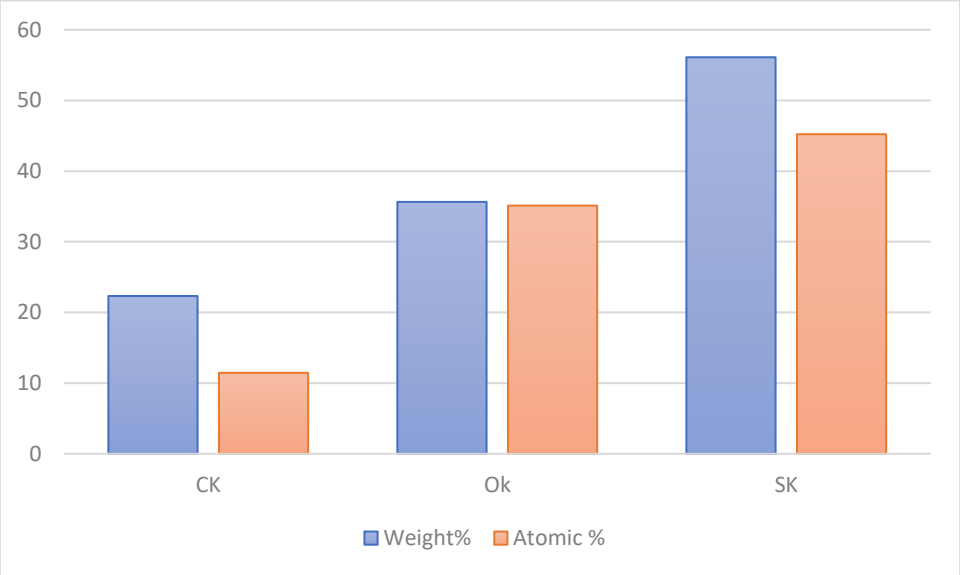

Figure 4 (b): Graphical representation on the percentage of Element Composition Analysis

CK, Ok, and SK weight and atomic percentages are shown by the data. Calcium and potassium (CK) have a weight percentage of 22.32% and an atomic percentage of 11.45%. This means that CK accounts for 11.45% of the sample's atoms and 22.32% of its weight. Ok, representing Oxygen and Potassium, has a weight percentage of 35.64% and an atomic percentage of 35.11%. Thus, Ok accounts for 35.64% of the sample's weight and 35.11% of its atomic makeup. Finally, for SK, the data shows 56.11% weight and 45.22% atomic. The sample's other elements are less abundant than SK in weight and atomic composition.

Table 1(c): Element Composition Analysis

Element	Weight%	Atomic %
CK	20.14	09.56
Ok	30.11	10.00
SK	45.22	54.11

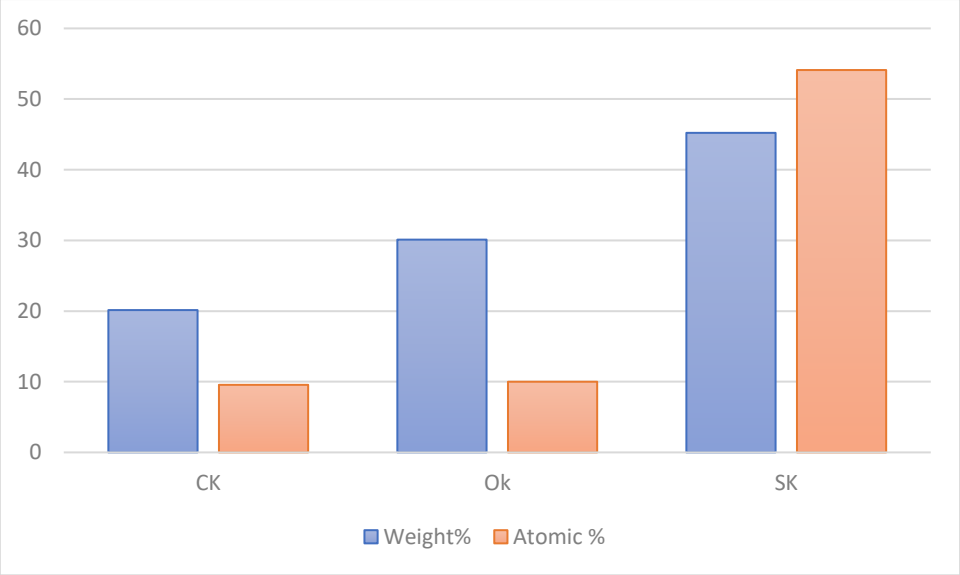

Figure 4(c): Graphical representation on the percentage of Element Composition Analysis

The analysis of three key elements in a sample reveals that Calcium and Potassium (CK) constitutes 20.14% of the total weight and 9.56% of the total number of atoms. Oxygen and Potassium (OK) account for 30.11% of the sample's weight and 10.00% of its atomic composition. Lastly, SK holds a significant presence in terms of weight and atomic composition, with a weight percentage of 45.22% and an atomic percentage of 54.11%. These data points highlight the importance of these elements in the sample's composition and weight.'

Table 1(d): Element Composition Analysis

Element	Weight%	Atomic %
CK	19.09	8.56
Ok	85.1	17.14
SK	41.20	21.32

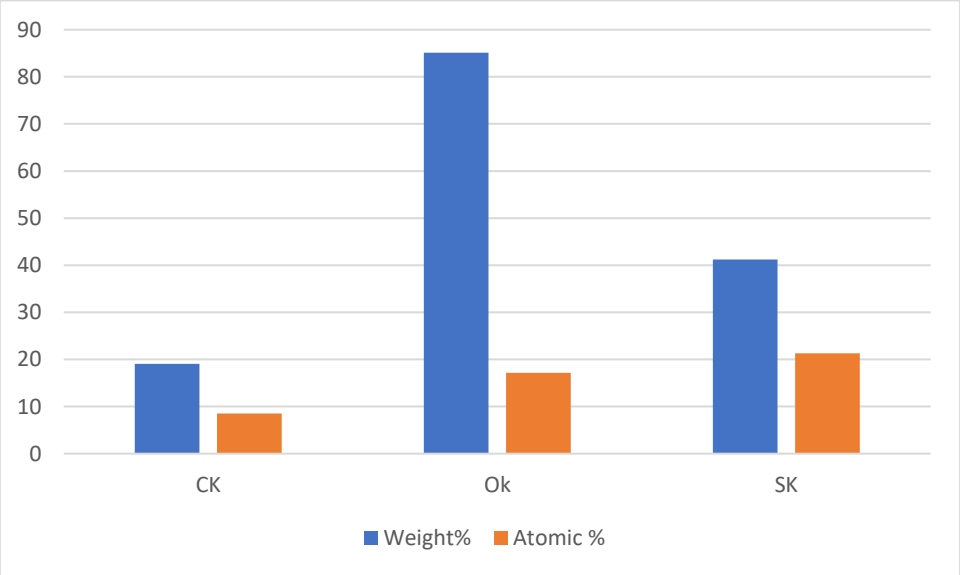

Figure 4 (d): Graphical representation on the percentage of Element Composition Analysis

The data shows the weight percentages and atomic percentages of three elemental components: CK, Ok, and SK. CK, representing Calcium and Potassium, has a weight percentage of 19.09% and an atomic presence of 8.56%. Ok, representing Oxygen and Potassium, has a weight percentage of 85.1% and an atomic percentage of 17.14%. Ok dominates the sample's weight composition significantly, contributing 85.1% and holding a significant share of its atomic composition at 17.14%. SK, with a weight percentage of 41.20% and an atomic percentage of 21.32%, has a notable presence in terms of weight and atomic composition.

4.3.Magnetic Properties

The review broke down the attractive ways of behaving of Fe3O4 nanoparticles and attractive hydrogel utilizing vibrating test magnetometry (VSM) at room temperature. The outcomes showed that both nanoparticles and attractive hydrogel displayed superparamagnetic and paramagnetic ways of behaving, individually. The charge capacity was affirmed when presented to an attractive field, however no long-lasting polarization existed after the field evacuation. The immaculate Fe3O4 nanoparticles showed instigated polarization of 60-65 emu/g at the level, while the paramagnetic hydrogel had actuated charge upsides of 0.6-0.66 and 1-1.04 emu/g. The outcomes showed a decrease in immersion polarization of M-St-g-PAA/CNFs contrasted with perfect Fe3O4, essentially because of the low happy of implanted and scattered Fe3O4 nanoparticles in the hydrogel lattice.

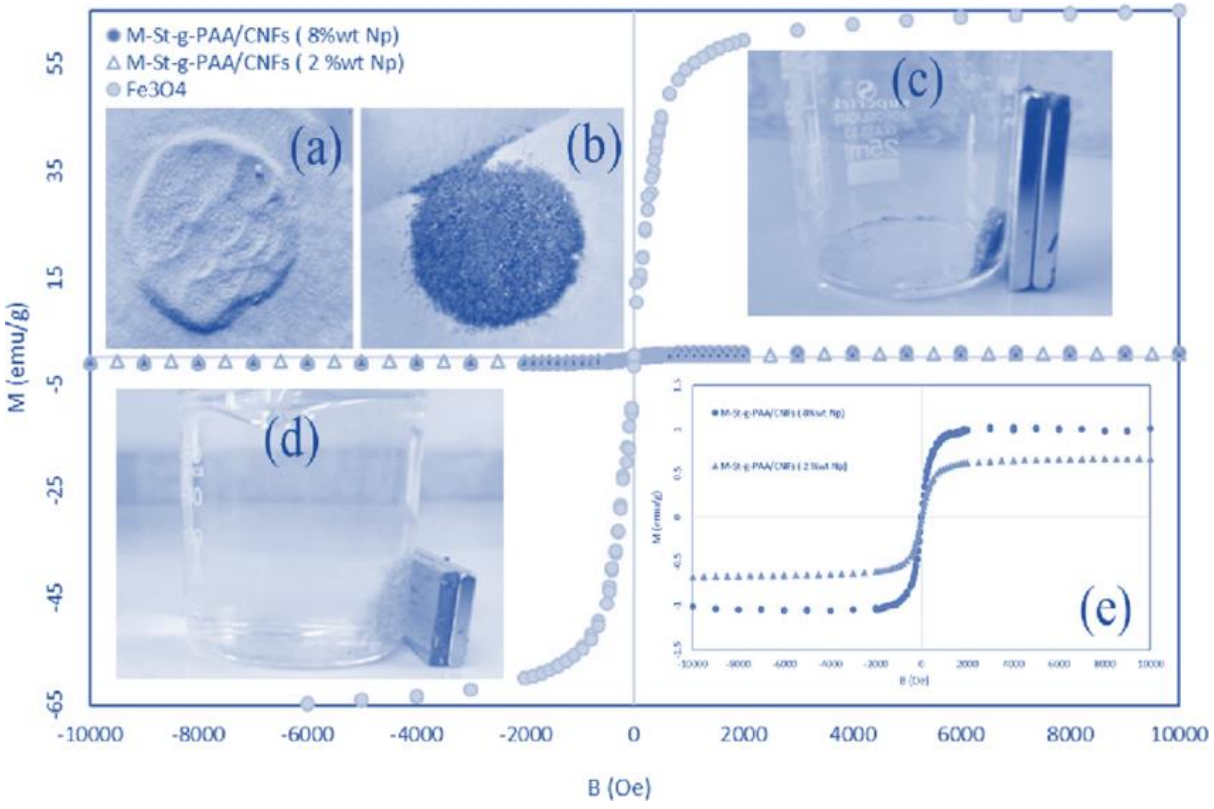

Figure 5. Pictures of (a) St-g-PAA/CNFs and (b) M-St-g-PAA/CNFs in powder structure; (c) an alluring hydrogel in dry structure and (d) an expanding structure in water made by an enduring magnet; and (e) a polarization plot (M) for Fe3O4 nanoparticles and the alluring hydrogel nanocomposite M-St-g-PAA/CNFs at room temperature as a part of the applied appealing field (B).

5. CONCLUSION

Promising outcomes for water treatment applications are uncovered by the amalgamation and characterisation of starch-g-poly(acrylic corrosive) (St-g-PAA) hydrogels supported with cellulose nanofibers (CNFs) for Cu2+ particle adsorption. The hydrogels' adsorption capacity, recuperation proficiency, and underlying respectability are totally worked on by the expansion of CNFs and attractive nanoparticles (Fe3O4). The hydrogel grid and Cu2+ particles' compound connections are affirmed by FTIR spectroscopy examination, and the morphological changes that happen during adsorption are portrayed in SEM photos. The basic cosmetics of the hydrogels and their connections with Cu2+ particles are additionally explained by component sythesis investigation. Moreover, the paramagnetic way of behaving of attractive hydrogels and the superparamagnetic conduct of Fe3O4 nanoparticles are shown by vibrating test magnetometry. In light of everything, these outcomes feature the capability of composite hydrogels as effective adsorbents for the expulsion of weighty metals from fluid arrangements, giving a drawn out method for diminishing water contamination and backing natural restoration drives. Resulting examinations might focus on refining the amalgamation boundaries and exploring the plausible execution of these hydrogels in genuine water treatment circumstances.

REFERENCES

1. Mandal S, Vishvakarma P. Nanoemulgel: A Smarter Topical Lipidic Emulsion-based Nanocarrier. Indian J of Pharmaceutical Education and Research. 2023;57(3s):s481-s498.
2. Mandal S, Jaiswal DV, Shiva K. A review on marketed Carica papaya leaf extract (CPLE) supplements for the treatment of dengue fever with thrombocytopenia and its drawback. International Journal of Pharmaceutical Research. 2020 Jul;12(3).
3. Mandal S, Bhumika K, Kumar M, Hak J, Vishvakarma P, Sharma UK. A Novel Approach on Micro Sponges Drug Delivery System: Method of Preparations, Application, and its Future Prospective. Indian J of Pharmaceutical Education and Research. 2024;58(1):45-63.
4. Mishra, N., Alagusundaram, M., Sinha, A., Jain, A. V., Kenia, H., Mandal, S., & Sharma, M. (2024). Analytical Method, Development and Validation for Evaluating Repaglinide Efficacy in Type Ii Diabetes Mellitus Management: a Pharmaceutical Perspective. Community Practitioner, 21(2), 29–37. https://doi.org/10.5281/zenodo.10642768
5. Singh, M., Aparna, T. N., Vasanthi, S., Mandal, S., Nemade, L. S., Bali, S., & Kar, N. R. (2024). Enhancement and Evaluation of Soursop (Annona Muricata L.) Leaf Extract in Nanoemulgel: a Comprehensive Study Investigating Its Optimized Formulation and Anti-Acne Potential Against Propionibacterium Acnes, Staphylococcus Aureus, and Staphylococcus Epidermidis Bacteria. Community Practitioner, 21(1), 102–115. https://doi.org/10.5281/zenodo.10570746
6. Khalilullah, H., Balan, P., Jain, A. V., & Mandal, S. (n.d.). EUPATORIUM REBAUDIANUM BERTONI (STEVIA): INVESTIGATING ITS ANTI-INFLAMMATORY POTENTIAL VIA CYCLOOXYGENASE AND LIPOOXYGENASE ENZYME INHIBITION - A COMPREHENSIVE MOLECULAR DOCKING AND ADMET. Community Practitioner, 21(03), 118–128. https://doi.org/10.5281/zenodo.10811642

7. Mandal, S. (n.d.). GENTAMICIN SULPHATE BASED OPHTHALMIC NANOEMULGEL: FORMULATION AND EVALUATION, UNRAVELLING A PARADIGM SHIFT IN NOVEL PHARMACEUTICAL DELIVERY SYSTEMS. Community Practitioner, 21(03). https://doi.org/10.5281/zenodo.10811540
8. Mandal, S., Tyagi, P., Jain, A. V., & Yadav, P. (n.d.). Advanced Formulation and Comprehensive Pharmacological Evaluation of a Novel Topical Drug Delivery System for the Management and Therapeutic Intervention of Tinea Cruris (Jock Itch). Journal of Nursing, 71(03). https://doi.org/10.5281/zenodo.10811676
9. Mishra, N., Alagusundaram, M., Sinha, A., Jain, A. V., Kenia, H., Mandal, S., & Sharma, M. (2024). Analytical Method, Development and Validation for Evaluating Repaglinide Efficacy in Type Ii Diabetes Mellitus Management: a Pharmaceutical Perspective. Community Practitioner, 21(2), 29–37. https://doi.org/10.5281/zenodo.10642768
10. Singh, M., Aparna, T. N., Vasanthi, S., Mandal, S., Nemade, L. S., Bali, S., & Kar, N. R. (2024). Enhancement and Evaluation of Soursop (Annona Muricata L.) Leaf Extract in Nanoemulgel: a Comprehensive Study Investigating Its Optimized Formulation and Anti-Acne Potential Against Propionibacterium Acnes, Staphylococcus Aureus, and Staphylococcus Epidermidis Bacteria. Community Practitioner, 21(1), 102–115. https://doi.org/10.5281/zenodo.10570746Pal N, Mandal S, Shiva K, Kumar B. Pharmacognostical, Phytochemical and Pharmacological Evaluation of Mallotus philippensis. Journal of Drug Delivery and Therapeutics. 2022 Sep 20;12(5):175-81.
11. Singh A, Mandal S. Ajwain (Trachyspermum ammi Linn): A review on Tremendous Herbal Plant with Various Pharmacological Activity. International Journal of Recent Advances in Multidisciplinary Topics. 2021 Jun 9;2(6):36-8.
12. Mandal S, Jaiswal V, Sagar MK, Kumar S. Formulation and evaluation of carica papaya nanoemulsion for treatment of dengue and thrombocytopenia. Plant Arch. 2021;21:1345-54.
13. Mandal S, Shiva K, Kumar KP, Goel S, Patel RK, Sharma S, Chaudhary R, Bhati A, Pal N, Dixit AK. Ocular drug delivery system (ODDS): Exploration the challenges and approaches to improve ODDS. Journal of Pharmaceutical and Biological Sciences. 2021 Jul 1;9(2):88-94.
14. Shiva K, Mandal S, Kumar S. Formulation and evaluation of topical antifungal gel of fluconazole using aloe vera gel. Int J Sci Res Develop. 2021;1:187-93.
15. Ali S, Farooqui NA, Ahmad S, Salman M, Mandal S. Catharanthus roseus (sadabahar): a brief study on medicinal plant having different pharmacological activities. Plant Archives. 2021;21(2):556-9.
16. Mandal S, Vishvakarma P, Verma M, Alam MS, Agrawal A, Mishra A. Solanum Nigrum Linn: An Analysis Of The Medicinal Properties Of The Plant. Journal of Pharmaceutical Negative Results. 2023 Jan 1:1595-600.
17. Vishvakarma P, Mandal S, Pandey J, Bhatt AK, Banerjee VB, Gupta JK. An Analysis Of The Most Recent Trends In Flavoring Herbal Medicines In Today's Market. Journal of Pharmaceutical Negative Results. 2022 Dec 31:9189-98.

18. Mandal S, Vishvakarma P, Mandal S. Future Aspects And Applications Of Nanoemulgel Formulation For Topical Lipophilic Drug Delivery. European Journal of Molecular & Clinical Medicine.;10(01):2023.
19. Chawla A, Mandal S, Vishvakarma P, Nile NP, Lokhande VN, Kakad VK, Chawla A. Ultra-Performance Liquid Chromatography (Uplc).
20. Mandal S, Raju D, Namdeo P, Patel A, Bhatt AK, Gupta JK, Haneef M, Vishvakarma P, Sharma UK. Development, characterization, and evaluation of rosa alba l extract-loaded phytosomes.